Asian Journal of Chemistry; Vol. 36, No. 2 (2024), 301-306

ASIAN JOURNAL OF CHEMISTRY

https://doi.org/10.14233/ajchem.2024.30308

Biosynthesis, Characterization and Antimicrobial Efficacy of Zinc Oxide Nanoparticles *via Plectranthus amboinicus* Leaf Extract

V. PORKALAI[1], N. LAVANYA[2], R. NITHYA[3] and R. SAGAYARAJ[4,*]

[1]PG & Research Department of Physics, Thiru.Vi.Ka. Government Arts College (Affiliated to Bharathidasan University), Thiruvarur-610003, India
[2]PG & Research Department of Physics, A.D.M. College for Women (Affiliated to Bharathidasan University), Nagapattinam-611001, India
[3]Department of Physics, Sanskrithi School of Engineering (Affiliated to Jawaharlal Nehru Technological University), Puttaparthi-515134, India
[4]PG & Research Department of Physics, St. Joseph's College of Arts and Science (Autonomous) (Affiliated to Annamalai University), Cuddalore-607001, India

*Corresponding author: E-mail: sagayarajnancy@gmail.com

Received: 18 September 2023; *Accepted*: 3 November 2023; *Published online*: 31 January 2024; AJC-21516

This study investigates the environmental friendly synthesis of zinc oxide nanoparticles using *Plectranthus amboinicus* leaf extract. The X-ray diffraction (XRD) analysis confirms the presence of well-crystalline ZnO nanoparticles with a crystallite size of 42 nm. Scanning electron microscopy (SEM) reveals the size, shape and distribution of nanoparticles within the extract, indicating their impact on *Plectranthus amboinicus* growth. Energy dispersive X-ray (EDX) analysis confirmed the high nanoparticle purity, while FTIR spectral analysis identifies the organic compounds involved in the synthesis. UV-visible absorption spectroscopy shows a reduced bandgap energy in the green-synthesized ZnO nanoparticles. Dynamic light scattering (DLS) analysis indicates a mean particle size of 11 nm with a significant stability. These nanoparticles exhibit exceptional antimicrobial activity, especially against Gram-negative bacteria. This eco-friendly synthesis method offers cost-effectiveness, safety and sustainability, promising diverse applications in the antimicrobial therapies, food preservation and water treatment, addressing various industrial challenges.

Keywords: ZnO, Nanoparticles, *Plectranthus amboinicus*, Green synthesis, Antibacterial activity.

INTRODUCTION

A particularly promising avenue involves the utilization of nanoparticles with zinc oxide nanoparticles emerging as a standout due to their potent antibacterial properties. Furthermore, there has been an increasing interest towards utilizing environmental friendly and sustainable green synthesis techniques for the production of nanoparticles [1]. Zinc oxide (ZnO) stands out as an exemplary semiconductor nanoparticle with a wide-bandgap and n-type properties, featuring an energy gap (E_g) of 3.37 eV. This unique bandgap value plays a pivotal role in defining the diverse and promising applications of ZnO in various fields [2-4]. With remarkable ultraviolet (UV) absorption capabilities, ZnO nanoparticles have emerged as a highly desirable ingredient in personal care products, encompassing cosmetics and sunscreens, effectively shielding the skin from the detrimental impacts of UV radiation [5]. Moreover, these nanoparticles demonstrate exceptional antibacterial, antimicrobial and UV blocking attributes, elevating their utility beyond the realm of skin care. In the textile industry, when incorporated into fabric production, ZnO NPs bestow finished fabrics with a plethora of enhanced functionalities, including heightened resistance against both ultraviolet and visible light, potent antibacterial properties and deodorizing prowess [6].

Zinc oxide (ZnO) nanoparticles have long been synthesized using various physical and chemical techniques. For example, sol-gel, coprecipitation and hydrothermal methods, while effective, often require high temperatures, pressures, expensive and toxic chemicals and non-polar solvents, posing significant challenges for materials researchers [7-9]. To overcome these obstacles, researchers have explored diverse chemical and physical approaches to produce nanoparticles of different crystallite sizes, morphology and compositions.

The synthesis of ZnO nanostructures can be accomplished through several methods. For instance, direct precipitation involves dissolving zinc compounds in water and subsequently allowing the solution to evaporate, leading to the precipitation of zinc oxide nanoparticles. On the other hand, homogeneous precipitation entails mixing inorganic salts with ligands such as amines to form ZnO nanoparticles [10,11]. Recently, there has been an increasing interest in the biological method of synthesizing ZnO nanoparticles, which offers simplicity, eco-friendly and significant antimicrobial activity. The studies in this area suggest that biological synthesis plays a significant role in shaping the future of ZnO nanoparticle production [12]. According to Kolekar *et al*. [13], eco-friendly biosynthesized nanoparticles should be used instead of chemically synthesized nanoparticles in order to reduce the toxicity of chemicals in the environment. The green synthesis of nanoparticles involves utilizing microorganisms and plants to synthesize nanoparticles, offering potential biomedical applications [14,15].

Green synthesis encompasses the synthesis of zinc oxide nanoparticles (ZnO NPs) using plants, bacteria, fungi and algae, enabling the generation of impurity-free ZnO NPs on a significant scale [16]. Nanoparticles synthesized *via* a biomimetic approach exhibit enhanced catalytic activity while reducing reliance on costly and hazardous chemicals. The biosynthesis of nanoparticles is a strategy involving microorganisms and plants, with potential biomedical applications [17]. The utilization of green synthesis techniques enables the efficient and extensive manufacturing of ZnO NPs without the presence of unwanted impurities. Additionally, green sources serve the dual purpose of stabilizing and reducing agents in the synthesis of nanoparticles with precise control over their shape and size [18].

Different researchers utilized different parts of different plants *e.g*. *Myristica fragrans* [19], *Elaeagnus angustifolia* [20], *Cassia fistula* [21], *Melia azedarach* [21], *Acalypha indica* [22], *Calotropis gigantean* [23], *Ocimum sanctum* [24], *Coriandrum sativum* [25], *Mussaenda frondosa* [26], *Eucalyptus globulus* Labill. [27], *Ocimum americanum* [28], *Trifolium pratense* [29], *Sambucus ebulus* [30], *Acalypha fruticosa* [31], *etc*. for the synthesis of ZnO nanoparticles. Thus, keeping in mind about the usefulness of the plants in the synthesis of metallic nanoparticles, this article presents a fascinating findings that explores the antibacterial properties of ZnO nanoparticles, which were synthesized by employing a green method including the use of *Plectranthus amboinicus* leaf extact. This ingenious process involves the preparation of the nanoparticles from naturally derived sources that are non-toxic, environmentally benign and cost-effective.

EXPERIMENTAL

High grade chemicals including zinc acetate dihydrate ($Zn(CH_3COO)_2{\cdot}2H_2O$) and all other reagents were procured from Merck Chemical Reagent Co. The distilled water used throughout the experimental work and the fresh leaves of *Plectranthus amboinicus* plant was collected from the local gardens in and around Nagapattinam, India.

Sample collection and authentication: Fresh leaves of *P. amboinicus* were carefully harvested in Nagapattinam city, India then gently cleaned with tissue paper. Subsequently, the leaves were authenticated by Department of Agriculture at Annamalai University, Annamalai Nagar, India. The collected leaves underwent thorough washing with tap water followed by multiple rinses with double-distilled water to remove any surface dust. These meticulously cleaned leaves were then shade-dried for 2 days.

Green synthesis of ZnO nanoparticles: The dried leaves were finely crushed and soaked in 100 mL of distilled water to extract the bioactive compounds. A zinc oxide precursor solution was prepared by dissolving zinc salts in a suitable solvent. The *P. amboinicus* leaf extract was then combined with the precursor solution and stirred at a controlled temperature. Over time, the reduction of zinc ions and the formation of ZnO nanoparticles occured.

Antibacterial activity: The different types of bacterial strains, encompassing both Gram-positive and Gram-negative categories were intentionally chosen based on their unique attributes to serve as models for the scientific experimentation. The standard agar well diffusion or broth microdilution method was commonly employed to determine the minimum inhibitory concentration (MIC) and zone of inhibition of the nanoparticles against the three bacterial strains *viz*. *Staphylococcus epidermidis*, *Escherichia coli* and *Bacillus subtilis*.

RESULTS AND DISCUSSION

XRD studies: The obtained XRD patterns (Fig. 1), exhibited the distinct diffraction peaks at precise angles, namely 28.39º, 29.41º, 31.41º, 34.46º, 36.17º, 40.59º, 47.46º, 56.48º, 62.73º, 66.26º, 67.83º, 68.94º, 72.54º and 76.92º, which corresponded to various crystallographic planes, including (100), (002), (101), (110), (102), (103), (112), (201) and (202). Importantly, these plane values aligned remarkably well with the wurtzite structure of ZnO as supported by the hexagonal wurtzite ZnO reflection lines (JCPDS card no. 36-1451) [32-34]. The distinct sharpness and intensity of these diffraction peaks provided compelling evidence of the well-crystalline nature of the

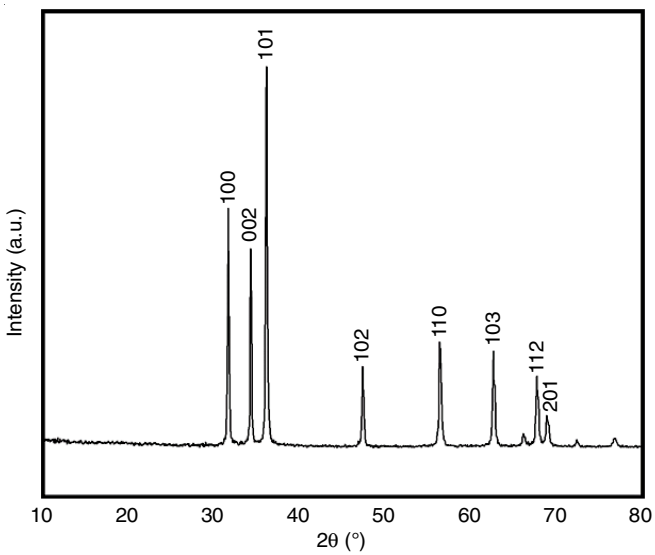

Fig. 1. XRD spectrum of biosynthesized ZnO nanoparticles

biosynthesized ZnO nanoparticles. To determine the crystallite size of the ZnO nanoparticles, the Scherrer's formula was employed (eqn. 1):

$$D = \frac{0.9\lambda}{\beta\cos\theta}$$

where D represents the particle size, λ denotes the wavelength of the utilized source (Cu, *K*α), β signifies the full-width at half maximum (FWHM) of the ZnO (101) line and θ corresponds to the diffracting angle. Interestingly, *P. amboinicus* was used to biosynthesized ZnO, which produced nanoparticles with a 42 nm crystallite size [19,29,31,33]. Table-1 showed particle sizes and properties of zinc oxide nanomaterials from diverse plant sources, which could be used in materials science and nanotechnology and biotechnology applications.

Morphological studies: The SEM analysis of ZnO nanoparticles in conjunction with *P. amboinicus* provides valuable insights into the particle's shape, size and crystallinity. Upon closer examination, the SEM image (Fig. 2) revealed that ZnO nanoparticles, when added to *P. amboinicus* leaf extract, exhibit a smaller size, typically around 1 µm. The morphology of these nanoparticles exhibits variation based on the concentration of ZnO in the extraction solution. Larger particle aggregates occur at higher concentrations and have ripple-like characteristics. Generally, the particles possess a smooth and homogeneous surface, although the occasional irregularities have been observed in Fig. 2. Occasionally, particles may be coated with an extra layer composed of organic materials. As a result, a spherical shaped nanoparticles and aggregated molecules were identified within *P. amboinicus* leaf extract [26].

EDX studies: Fig. 3 displays the EDX spectrum of the biosynthesized ZnO nanoparticles, which reveals their composition. Regarding the composition, the weight percentages of zinc (Zn) and oxygen (O) in the sample stand at 77.5% and 22.5%, respectively. Additionally, the atomic percentages of these elements were measured at 54.3% for Zn and 45.7% for O, affirming the absence of significant impurities in the biosynthesized ZnO nanoparticles [27].

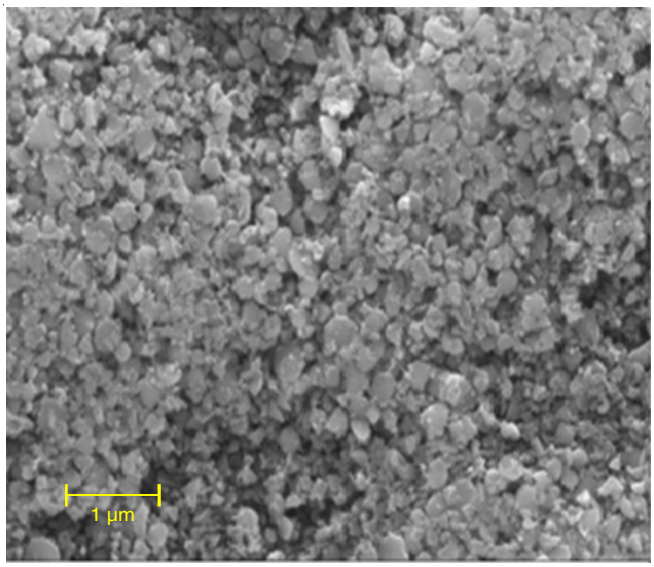

Fig. 2. SEM image of biosynthesized ZnO nanoparticles

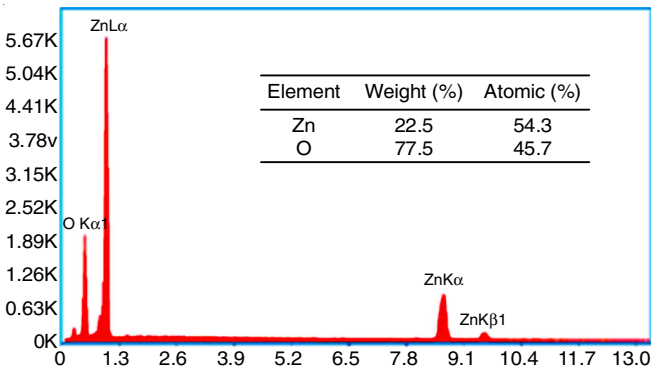

Fig. 3. EDX spectrum of biosynthesized ZnO nanoparticles

TABLE-1
DATA ON ZnO NPs AGAINST DIFFERENT LEAF OR FRUIT EXTRACT

Materials	Leaf/fruit extract	Crystallite size	Absorbance band, Bandgap energy	DLS, zeta potential	Ref.
Zinc oxide (ZnO)	*Myristica fragrans*	41.23 nm	2.57 eV	66 nm and ?22.1 mV	[19]
Zinc nitrate hexahydrate	*Elaeagnus angustifolia*	29 nm	399 nm	205.9 nm, ZP of 13.8 mV and PDI of 0.132	[20]
Zinc oxide (ZnO)	*Cassia fistula* and *Melia azadarach*	2.72 nm	320 and 324 nm	3 to 68 nm	[21]
Zinc acetate dihydrate	*Acalypha indica*	16 nm	3.34 eV	46 nm and -27 mV	[22]
Zinc acetate dihydrate	*Calotropis gigantean*	10 nm	350 nm	11 nm (100%)	[23]
Zinc acetate dihydrate	*Ocimum sanctum*	18, 12 and 17 nm	3.32-3.20 eV	-24.86, -26.48 and -23.19 mV	[24]
Zinc oxide	*Coriandrum sativum*	60 nm	3.8 eV	55 nm	[25]
Zinc oxide	*Mussaenda frondosa*	5 and 20 nm	3.33, 3.27 and 3.30 eV	+ 30 and -30 mV	[26]
Zinc oxide	*Eucalyptus globulus* Labill.	27 and 35 nm	2.67 eV	-40 mV	[27]
Zinc oxide	*Ocimum americanum*	21 nm	316 nm	21 nm, 12.6 mV	[28]
Zinc oxide (ZnO)	*Trifolium pratense*	60-70 nm	283 nm	8.63 keV	[29]
Zinc oxide	*Sambucus ebulus*	17 nm	350 nm 3.3 eV		[30]
ZnO (zinc acetate dehydrate)	*Acalypha fruticosa*	40 nm	310 nm		[31]
Zinc oxide	*Plectranthus amboinicus* plant	42 nm	377 nm/3.66 eV	11 nm, 0.375 PDLi, -3 mV	Present study

FTIR studies: The FTIR spectrum of ZnO nanoparticles was recorded within the 4000-500 cm^{-1} range as shown in Fig. 4. The presence of Zn-O has been firmly identified by a distinct peak in the range of 600-400 cm^{-1}. Upon further closer examination of the spectrum, distinct peaks are also observed at 3406, 2925, 1362 and 481 cm^{-1}. The band observed at 481 cm^{-1} may be attributed to the stretching vibrations of ZnO, confirming the existence of ZnO within the nanoparticle structure. Simultaneously, the broad band at 3406 cm^{-1} exhibits the characteristic peak of hydroxyl groups (O–H), indicating the participation of molecules containing hydroxyl groups in the synthetic process. Another significant broad peak at 1362 cm^{-1} indicates the stretching of –C–O bonds, which suggests the existence of compound that contain carbon-oxygen bonds, such as esters, carboxylic acids or ethers. The presence of C-C bonds in the biosynthesized ZnO nanoparticles is indicated by the peak observed at 2925 cm^{-1}, which can be attributed to –C–C– stretching vibrations. The presence of a broad absorbance peak at 3406 cm^{-1} indicates the co-existence of various organic components, such as alcohols, aldehydes and ketones (C=O stretching), alkenes, nitro groups (N=O bending), esters, carboxylic acids, or ethers (C-O stretching) and alkyl halides. Thus, the presence of the wide range of organic chemicals suggests their use in ZnO nanoparticle synthesis. Interestingly, the presence of organic compounds such as flavonoids or terpenoids in the leaf extract appears to play a pivotal role in the synthesis process, while proteins present in the extract contribute to the stabilization of the ZnO nanoparticles, forming a protective coating around them [28]. This synergistic action highlights the complex and dynamic mechanisms involved in ZnO NPs formation and stability, improving our understanding of their potential uses.

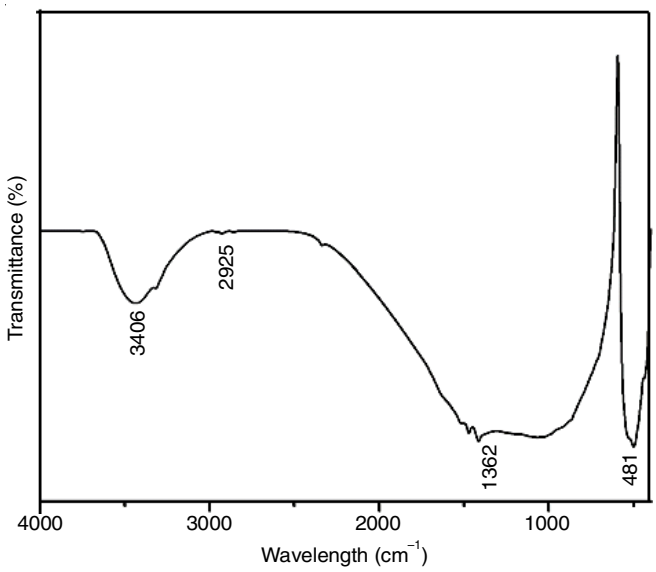

Fig. 4. FTIR spectrum of biosynthesized ZnO nanoparticles

UV-visible studies: A prominent UV-vis absorption peak at 377 nm is observed (Fig. 5), alongside a bandgap value of 3.66 eV, indicating significant electron transitions from the valence band to the conduction band. These findings strongly implied that the green synthesis of ZnO nanoparticles using plant extracts leads to a reduced bandgap energy [29], where the absorption spectra of ZnO nanoparticles fell within the range of 330 to 370 nm. Certain plant compounds that were incorporated into the ZnO lattice sites altered the electronic structure of the material, leading to a decrease in bandgap energy.

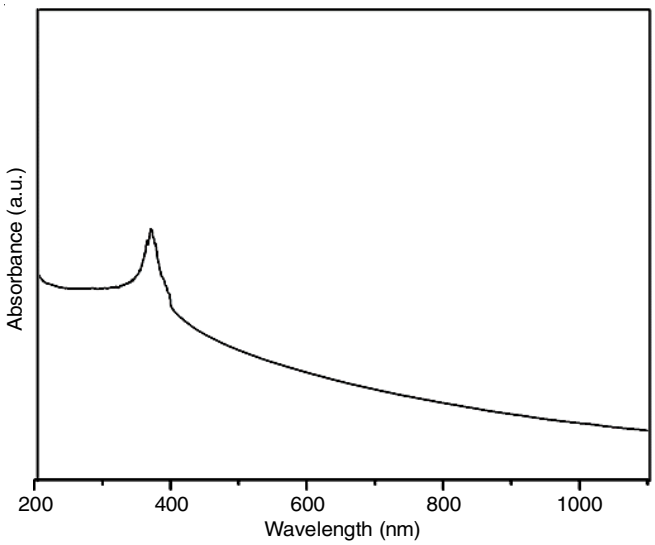

Fig. 5. UV-Vis spectrum of biosynthesized ZnO nanoparticles

DLS studies: The effectiveness of the eco-friendly green synthesis process depends on the exact control of parameters such as temperature, pH and pressure, ensuring that the resultant particles have the proper size, shape and distribution. These qualities can be verified by performing DLS-analysis, as shown in Fig. 6. The DLS-analyzed size of the synthesized ZnO nanoparticles reveals a mean size of 11 nm (100%) with a polydispersity index of 0.375 (PDI) [30]. Moreover, in Fig. 7, the zeta potential value of the biosynthesized ZnO nanoparticles in the colloidal solution is displayed. These nanoparticles exhibit a negative zeta potential value of -3 mV at room temperature, which provoke a remarkable stability due to the electrostatic repulsion. The robust negative charge confirms effective particle repulsion, sustaining the stability of these negatively charged nanoparticles. The assessment of zeta potential relies on observing the movement of nanoparticles when subjected to an applied

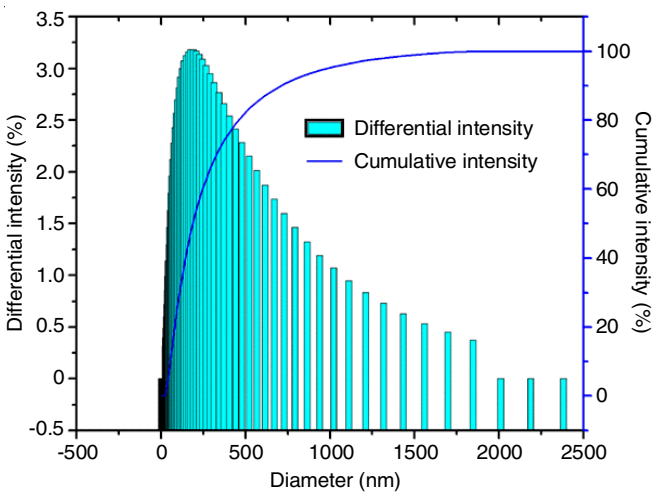

Fig. 6. DLS spectrum of biosynthesized ZnO nanoparticles

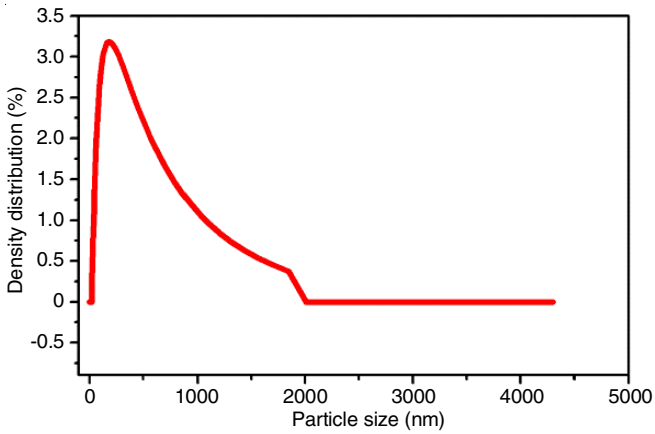

Fig. 7. Zeta potential curve of biosynthesized ZnO nanoparticles

electric field, which, in turn, depends on the surface charge and the local environment of the particles [31].

Antimicrobial activity: The ZnO nanoparticles produced through an environmental friendly green synthetic method were tested against three bacterial strains *e.g*. *Staphylococcus epidermidis*, *Escherichia coli* and *Bacillus subtilis*. The zone of inhibition values (Table-2) clearly illustrated the remarkable efficacy of biosynthesized ZnO NPs. The green-synthesized ZnO nanoparticles were particularly successful in inhibiting bacterial growth, which was likely due to their large surface area, which allowed them to effectively interact with the microbial cells. The biosynthesized ZnO nanoparticles have strong anti-bacterial action against Gram-negative bacteria suggesting they could treat Gram-negative diseases [35]. These results clearly revealed that *E. coli* is more affected than *B. subtilis* and *S. epidermidis* exploration for scientific and industrial communities alike.

TABLE-2
ANTIBACTERIAL ACTIVITY OF
ZnO NPs AGAINST DIFFERENT BACTERIA

Bacteria name	Zone of inhibition (diameter, mm)		
	Control	Standard*	P
Bacillus subtilis	–	24	14
Escherichia coli	–	23	15
Staphylococcus epidermidis	–	20	11

Conclusion

The synthesis and characterization of green-synthesized ZnO nanoparticles using *Plectranthus amboinicus* leaf extract have been successfully conducted in this study. The XRD analysis confirmed the crystalline nature of the nanoparticles, validating the presence of ZnO. The SEM analysis provided valuable insights into the particle's size, shape and distribution within the extract, while EDX analysis verified the high purity of the prepared ZnO nanoparticles. FTIR analysis identified the presence of various organic compounds involved in the synthesis process, shedding light on the complexity of the nanoparticle formation and stability. UV-Visible absorption spectroscopy revealed a reduced bandgap energy in the green-synthesized ZnO nanoparticles, indicating their potential for various electronic and optoelectronic applications. DLS analysis demonstrated the nanoparticles' mean size and remarkable stability due to the negative zeta potential, further enhancing their suitability for various applications. Additionally, the bio-synthesized ZnO nanoparticles exhibited exceptional anti-bacterial activity, especially against Gram-negative bacteria, positioning them as a promising solution for antimicrobial therapies, food preservation and water treatment.

ACKNOWLEDGEMENTS

The authors express their heartfelt gratitude to St. Joseph's College of Arts and Science (Autonomous) for generously granting access to the research laboratory and library facilities.

CONFLICT OF INTEREST

The authors declare that there is no conflict of interests regarding the publication of this article.

REFERENCES

1. R.S. Prakasham, B.S. Kumar, Y.S. Kumar and K.P. Kumar, *Indian J. Microbiol.*, **54**, 329 (2014); https://doi.org/10.1007/s12088-014-0452-1
2. I. Ayoub, V. Kumar, R. Abolhassani, R. Sehgal, V. Sharma, R. Sehgal, H.C. Swart and Y.K. Mishra, *Nanotechnol. Rev.*, **11**, 575 (2022); https://doi.org/10.1515/ntrev-2022-0035
3. D.K. Sharma, S. Shukla, K.K. Sharma and V. Kumar, *Mater. Today Proc.*, **49**, 3028 (2022); https://doi.org/10.1016/j.matpr.2020.10.238
4. V. Porkalai, D.B. Anburaj, B. Sathya, G. Nedunchezhian and R. Meenambika, *J. Mater. Sci. Mater. Electron.*, **28**, 2521 (2017); https://doi.org/10.1007/s10854-016-5826-1
5. Z. Fan and J.G. Lu, *J. Nanosci. Nanotechnol.*, **5**, 1561 (2005); https://doi.org/10.1166/jnn.2005.182
6. M.D. Newman, M. Stotland and J.I. Ellis, *J. Am. Acad. Dermatol.*, **61**, 685 (2009); https://doi.org/10.1016/j.jaad.2009.02.051
7. A. Hatamie, A. Khan, M. Golabi, A.P.F. Turner, V. Beni, W.C. Mak, A. Sadollahkhani, H. Alnoor, B. Zargar, S. Bano, O. Nur and M. Willander, *Langmuir*, **31**, 10913 (2015); https://doi.org/10.1021/acs.langmuir.5b02341
8. S. Makhluf, R. Dror, Y. Nitzan, Y. Abramovich, R. Jelinek and A. Gedanken, *Adv. Funct. Mater.*, **15**, 1708 (2005); https://doi.org/10.1002/adfm.200500029
9. L. Zhang, Y. Jiang, Y. Ding, M. Povey and D. York, *J. Nanopart. Res.*, **9**, 479 (2007); https://doi.org/10.1007/s11051-006-9150-1
10. M. Singh, S. Manikandan and A.K. Kumaraguru, *Res. J. Nanosci. Nanotech.*, **1**, 1 (2011); https://doi.org/10.3923/rjnn.2011.1.11
11. S. Ahmed, M. Ahmad, B.L. Swami and S. Ikram, *J. Adv. Res.*, **7**, 17 (2016); https://doi.org/10.1016/j.jare.2015.02.007
12. J. Rouhi, S. Mahmud, N. Naderi, C.R. Ooi and M.R. Mahmood, *Nanoscale Res. Lett.*, **8**, 364 (2013); https://doi.org/10.1186/1556-276X-8-364
13. T.V. Kolekar, S.S. Bandgar, S.S. Shirguppikar and V.S. Ganachari, *Arch. Appl. Sci. Res.*, **5**, 20 (2013).
14. S. Ying, Z. Guan, P.C. Ofoegbu, P. Clubb, C. Rico, F. He and J. Hong, *Environ. Technol. Innov.*, **26**, 102336 (2022); https://doi.org/10.1016/j.eti.2022.102336
15. A. Mahanty, S. Mishra, R. Bosu, U.K. Maurya, S.P. Netam and B. Sarkar, *Indian J. Microbiol.*, **53**, 438 (2013); https://doi.org/10.1007/s12088-013-0409-9
16. H. Agarwal, S. Venkat Kumar and S. Rajeshkumar, *Resour.-Effic. Technol.*, **3**, 406 (2017); https://doi.org/10.1016/j.reffit.2017.03.002
17. H.A. Salam, R. Sivaraj and R. Venckatesh, *Mater. Lett.*, **131**, 16 (2014); https://doi.org/10.1016/j.matlet.2014.05.033

18. R. Yuvakkumar, J. Suresh, A.J. Nathanael, M. Sundrarajan and S.I. Hong, *Mater. Sci. Eng. C*, **41**, 17 (2014); https://doi.org/10.1016/j.msec.2014.04.025
19. S. Faisal, H. Jan, S.A. Shah, S. Shah, A. Khan, M.T. Akbar, M. Rizwan, F. Jan, Wajidullah, N. Akhtar, A. Khattak and S. Syed, *ACS Omega*, **6**, 9709 (2021); https://doi.org/10.1021/acsomega.1c00310
20. J. Iqbal, B.A. Abbasi, T. Yaseen, S.A. Zahra, A. Shahbaz, S.A. Shah, S. Uddin, X. Ma, B. Raouf, S. Kanwal, W. Amin, T. Mahmood, H.A. El-Serehy and P. Ahmad, *Sci. Rep.*, **11**, 20988 (2021); https://doi.org/10.1038/s41598-021-99839-z
21. M. Naseer, U. Aslam, B. Khalid and B. Chen, *Sci. Rep.*, **10**, 9055 (2020); https://doi.org/10.1038/s41598-020-65949-3
22. G. Kamarajan, D.B. Anburaj, V. Porkalai, G. Nedunchezhian, A. Muthuvel and N. Mahendra, *J. Water Environ. Nanotechnol.*, **7**, 180 (2022); https://doi.org/10.22090/jwent.2022.02.006
23. S.K. Chaudhuri and L. Malodia, *Appl. Nanosci.*, **7**, 501 (2017); https://doi.org/10.1007/s13204-017-0586-7
24. R.M.I. Elsamra, M.S. Masoud, A.A. Zidan, G.M. El Zokm and M.A. Okbah, *Biomass Conv. Bioref.*, (2023); https://doi.org/10.1007/s13399-022-03709-1
25. P. Srinivasan and S. Mehtre, *Materials Today: Proc.*, **51**, 1760 (2022); https://doi.org/10.1016/j.matpr.2021.01.760
26. M.D. Jayappa, C.K. Ramaiah, M.A.P. Kumar, D. Suresh, A. Prabhu, R.P. Devasya and S. Sheikh, *Appl. Nanosci.*, **10**, 3057 (2020); https://doi.org/10.1007/s13204-020-01382-2
27. A.A. Barzinjy and H.H. Azeez, *SN Appl. Sci.*, **2**, 991 (2020); https://doi.org/10.1007/s42452-020-2813-1
28. H.K. Narendra Kumar, N.C. Mohana, B.R. Nuthan, K.P. Ramesha, D. Rakshith, N. Geetha and S. Satish, *SN Appl. Sci.*, **1**, 651 (2019); https://doi.org/10.1007/s42452-019-0671-5
29. R. Dobrucka and J. Dlugaszewska, *Saudi J. Biol. Sci.*, **23**, 517 (2016); https://doi.org/10.1016/j.sjbs.2015.05.016
30. S. Alamdari, M. Sasani Ghamsari, C. Lee, W. Han, H.-H. Park, M.J. Tafreshi, H. Afarideh and M.H.M. Ara, *Appl. Sci.*, **10**, 3620 (2020); https://doi.org/10.3390/app10103620
31. S. Vijayakumar, P. Arulmozhi, N. Kumar, B. Sakthivel, S. Prathip Kumar and P.K. Praseetha, *Mater. Today Proc.*, **23**, 73 (2020); https://doi.org/10.1016/j.matpr.2019.06.660
32. H. Hameed, A. Waheed, M.S. Sharif, M. Saleem, A. Afreen, M. Tariq, A. Kamal, W.A. Al-Onazi, D.A. Al Farraj, S. Ahmad and R.M. Mahmoud, *Micromachines*, **14**, 928 (2023); https://doi.org/10.3390/mi14050928
33. G. Kamarajan, D.B. Anburaj, V. Porkalai, A. Muthuvel and G. Nedunchezhian, *J. Nig. Soc. Phys. Sci.*, **4**, 892 (2022); https://doi.org/10.46481/jnsps.2022.892
34. S.P. Goutam, A.K. Yadav and A.J. Das, *J. Nanosci. Technol.*, **3**, 249 (2017).
35. S. Udhayan, R. Udayakumar, R. Sagayaraj and K. Gurusamy, *BioNanoSci.*, **11**, 703 (2021); https://doi.org/10.1007/s12668-021-00864-z